GEOLOGICA CARPATHICA, FEBRUARY 2009, 60, 1, 3–14 doi: 10.2478/v10096-009-0003-6

Ti-in-biotite geothermometry in non-graphitic, peraluminous metapelites from Crni vrh and Resavski humovi (Central Serbia)

SUZANA ERIĆ[1], MIHOVIL LOGAR[1], DRAGAN MILOVANOVIĆ[1], DANILO BABIČ[1] and BORIVOJ ADNAĐEVIĆ[2]

[1]Faculty of Mining and Geology, University of Belgrade, Đušina 7, Belgrade, Serbia; suzanaeric@yahoo.com
[2]Faculty of Physical Chemistry, University of Belgrade, Studenski trg 12–16, Belgrade, Serbia

(Manuscript received August 16, 2007; accepted in revised form June 12, 2008)

Abstract: The study discusses the application of the Ti-in-biotite geothermometer of Henry et al. (2005) to the example of biotites from non-graphitic peraluminous micaschists of Central Serbia. Three petrographically different micaschists were distinguished on the basis of the following mineral assemblages: CV1 (St-Grt-Bt-Ms-Pg-Pl-Qtz), CV2 (Grt-St-Ky-Bt-Ms-Pl-Qtz) and RH (Grt-St-Bt-Ms-Pl-Qtz). Applying different geothermobarometers it was estimated that the studied micaschists were metamorphosed at average temperatures and pressures of 530 °C and 520 MPa ($CV1_{incl}$), 580 °C and 670 MPa (CV1), 630 °C and 700 MPa (CV2) and 550 °C, 680 MPa (RH). The average temperatures obtained by the Ti-in-biotite method revealed uniform values for CV1 and CV2 micaschists and these values are very similar to the temperatures obtained by other methods. In contrast, the application of Ti-in-biotite geothermometer for RH micaschist yields the temperature difference of 85–110 °C. The variability of temperature is interpreted as a result of a positive correlation of Ti contents and X_{Mg} values in RH biotite, which is in disagreement with the principles of the Ti-in-biotite method. The positive Ti-X_{Mg} correlation is a result of the compositional variability shown by RH biotites from different samples, which can possibly be related to compositional inhomogeneities of the pelitic protolith. On the other hand, the Ti-in-biotite geothermometer for CV2 biotite gave very uniform temperatures despite variable Ti contents (Ti = 0.260, sd = 0.018 apfu). This is explained as result of the low sensitivity of Ti-in-biotite geothermometer for high Ti concentrations (> 0.25 apfu).

Key words: Serbia, Ti-in-biotite geothermometer, micaschists, non-graphitic metapelite.

Introduction

Along with the commonly used geothermometer based on Mg-Fe exchange between coexisting garnet and biotite (Ferry & Spear 1978; Perchuk & Lavrenteva 1983; Bhattacharya et al. 1992; Holldaway 2000) or the THERMOCALC program (Powell & Holland 2001), the amount of Ti in biotite could also be used to determine the temperature of metamorphism in metapelites (Henry et al. 2005). Experimental work on phlogopites has shown that there is a positive correlation between the amount of Ti in biotite and temperature and a negative correlation with pressure (Forbes & Flower 1974; Robert 1976).

Henry et al. (2005), suggested that geothermometric calculations based on the amount of Ti and Mg/(Mg + Fe) ratio in biotite can be applied to graphitic peraluminous metapelites that contain rutile and/or ilmenite and have equilibrated at pressures and temperatures of about 400–600 MPa and 480–800 °C, respectively. The authors suggest that this method can produce considerable disagreements with reference temperatures when it is applied to non-graphitic peraluminous metapelites containing Ti-saturated minerals. This paper aims to shed more light on this problem by investigating biotites from the micaschists in Serbia.

Micaschists from Crni vrh and Resavski humovi, associated with other metamorphic rocks in Proterozoic to Upper Paleozoic Crystalline Complexes in Central Serbia (Vujisić et al. 1981), correspond to non-graphitic peraluminous metapelites containing Ti-saturated minerals.

The geothermometer of Henry et al. (2005) is most sensitive for Ti contents in the range 0.0–0.3 apfu (atoms per formula unit). Biotites from the micaschists of Crni vrh and Resavski humovi, which have such a range of Ti content and are characterized by different X_{Mg} values 0.65), provide a good basis for discussing the applicability and sensitivity of the Ti-in-biotite geothermometer on non-graphitic peraluminous metapelites.

Geological setting

Micaschists of Crni vrh are exposed about 10 km southwest from Bagrdan, on the road between Strižilo and Donje Komarice villages, as well as along the Pišljak and Kusača streams (Fig. 1). Micaschists from Resavski humovi occur in the area around Miljko's monastery. The investigated micaschists are exposed as 10 to 40 m long outcrops, where these rocks are associated with amphibolites and pegmatites (Resavski humovi), or alternate with quartzites and gneisses (Crni vrh).

Geotectonically, the metamorphic rocks of Crni vrh and Resavski humovi belong to the northern and northwestern parts of the Serbo-Macedonian Composite Terrane (Karamata & Krstić 1996). The metamorphic rocks of the Serbo-Macedonian Massif were affected by polyphase metamorphism. According to

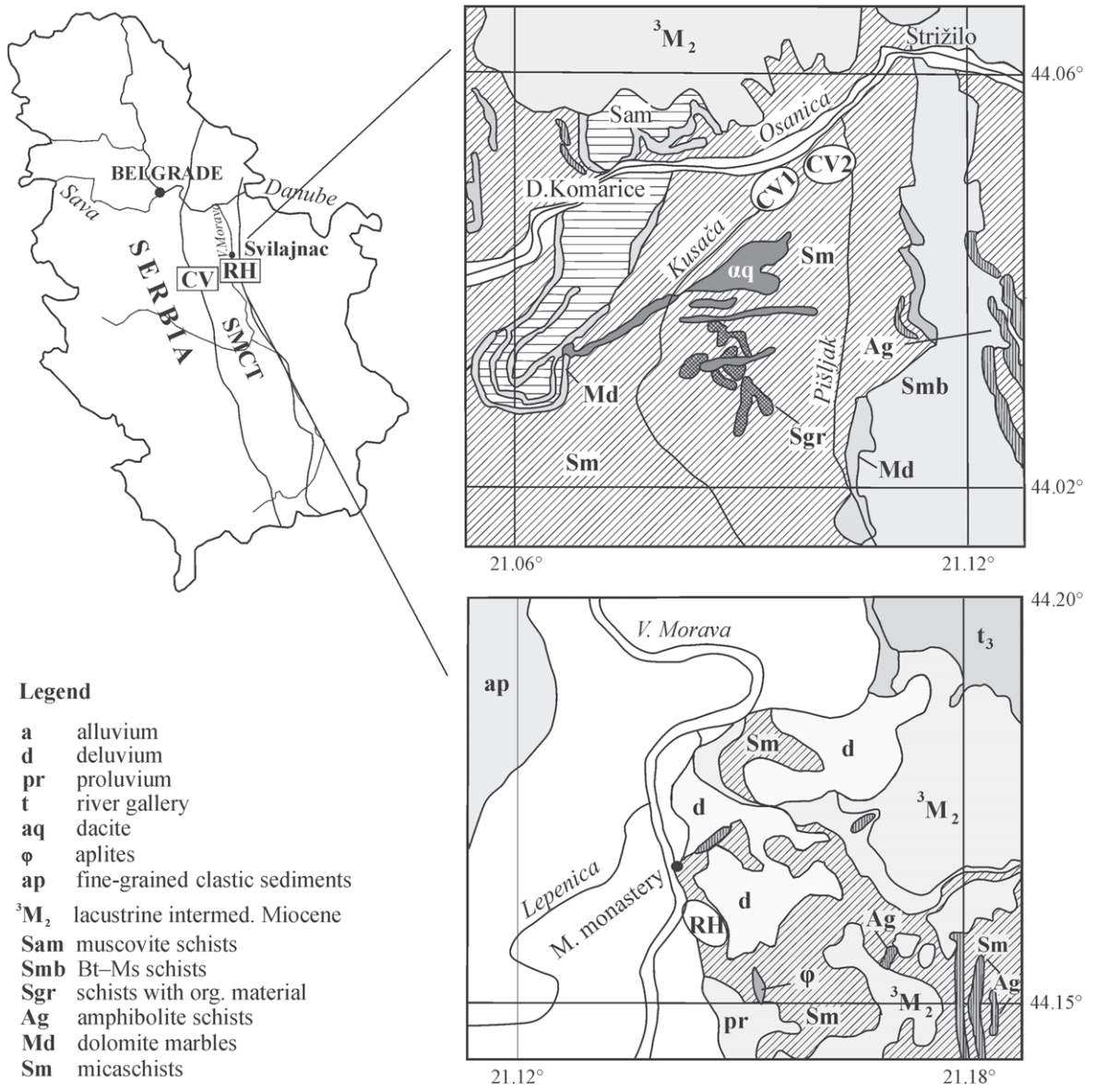

Fig. 1. Geological map of the Crni vrh and Resavski humovi in Central Serbia (Vujisić et al. 1979).

geochronological studies, these rocks were metamorphosed under amphibolite-, locally eclogite-facies conditions during the Caledonian and Hercynian events and underwent an Alpine overprint in greenschist-facies conditions (Balogh et al. 1994; Milovanović et al. 1998). They comprise wide variations of ortho- and paragneisses, micaschists and rarely marbles, amphibolites and eclogites. Gneisses and micaschists are most abundant. In places, gneisses and micaschists contain smaller bodies of amphibole gneisses, amphibolites, eclogites, marbles, or migmatitic patches and veins of quartz, feldspars and micas.

Petrography

Two different varieties of micaschists from Crni vrh (CV1 and CV2) and one of Resavski humovi (RH) are petrographically distinguished, mostly according to the amount and size of staurolite and garnet porphyroblasts and on the basis of the presence and absence of kyanite (Table 1). Micaschists of Crni vrh are composed of quartz, muscovite, biotite, sodic plagioclase, garnet, staurolite, kyanite and rarely of alkali feldspar. Tourmaline, rutile and ilmenite occur as accessory

Table 1: Mineral associations of micaschists from Crni vrh and Resavski humovi.

Micaschists from Crni vrh	Micaschists from Resavski humovi
St + Grt + Bt + Ms + Pg + Pl + Qtz (CV1) Grt + St + Ky + Bt + Ms + Pl + Qtz (CV2)	Grt + St + Bt + Ms + Pl + Qtz (RH)
Grt — garnet, St — staurolite, Ky — kyanite, Bt — biotite, Ms — muscovite, Pg — paragonite, Pl — plagioclase, Qtz — quartz	

Fig. 2. First variety of micaschist from Crni vrh (CV1).

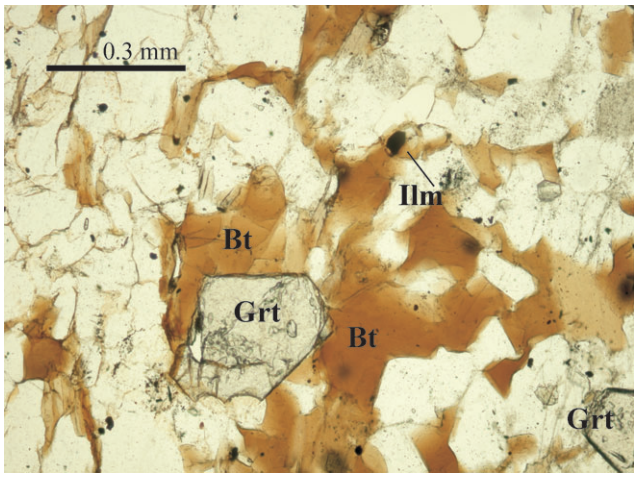

Fig. 3. Garnet porphyroblasts from CV1, N ∥. **Grt** — garnet, **Bt** — biotite, **Ilm** — ilmenite.

Fig. 4. Second variety of micaschist from Crni vrh (CV2).

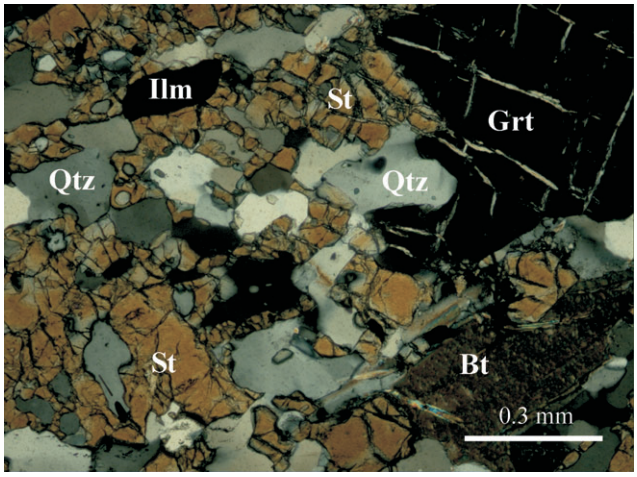

Fig. 5. Staurolite and garnet from CV2, N+. **St** — staurolite, **Qtz** — quartz, **Grt** — garnet, **Bt** — biotite.

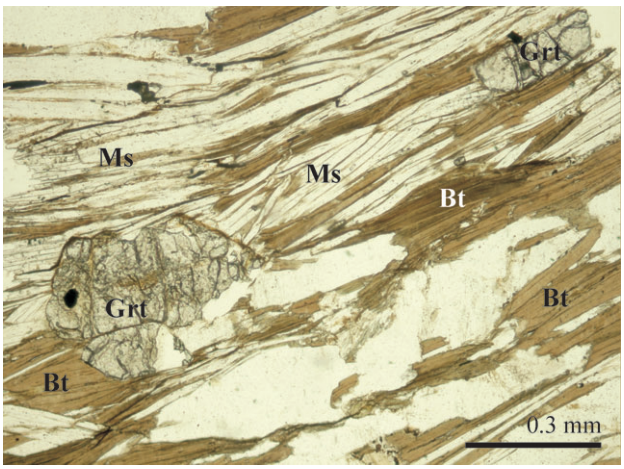

Fig. 6. Garnet with micas from RH, N ∥. **Bt** — biotite, **Ms** — muscovite, **Grt** — garnet.

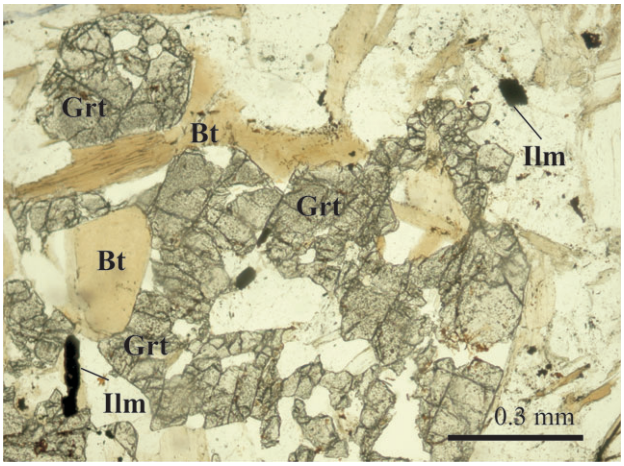

Fig. 7. Garnet and biotite from RH, N ∥. **Bt** — biotite, **Grt** — garnet, **Ilm** — ilmenite.

minerals. CV1 micaschist contains very large staurolite porphyroblasts as idiomorphic (Fig. 2), rarely hypidiomorphic grains up to 10 cm in size, which compose nearly 25 vol. % of the rock. These porphyroblasts contain frequent inclusions of garnet, biotite, muscovite, plagioclase and quartz. Garnet occurs either as inclusions or porphyroblasts up to 0.4 cm in diameter (Fig. 3). Paragonite has been observed in the groundmass along with muscovite and biotite. The dominant mineral of CV2 micaschist is garnet appearing as large, idiomorphic porphyroblasts up to 1 cm in diameter (Fig. 4), while staurolite (Fig. 5) and kyanite porphyroblasts, ranging in size from 0.5 mm to 0.5 cm, are less abundant.

Micaschists from Resavski humovi (RH) consist of quartz, micas (biotite and muscovite, Fig. 6), sodic plagioclase, garnet and staurolite. Garnet appears as large (up to 0.7 cm in diameter), idiomorphic porphyroblasts usually containing inclusions of muscovite and quartz.

In all the micaschist varieties biotite is texturally associated with muscovite. It occurs as orientated flakes and sheet-like aggregates defining the main rock fabric characterized by a pronounced schistosity. In some samples the micas build patches or bands up to a few mm in thickness. These mica-rich bands sometimes alternate with quartz aggregates producing a banded structure. Flakes of micas are up to 2 mm, commonly from 0.3 to 1 mm in length (Fig. 7). Besides the matrix biotite, tiny biotite flakes (from 0.05 to 0.3 mm in size) included in staurolite porphyroblasts were also observed in the CV1 micaschist variety.

Analytical methods

The mineral chemistry of micaschists from both localities was obtained using an EMPA, CAMECA, SX 100 electron microprobe at the Institute of Mineralogy and Petrography, University of Hamburg, Germany. Operating conditions were 15 kV accelerating voltage and 20 nA sample current. Four representative samples were taken from each micaschist variety. More than 100 microprobe analyses of biotite and a similar number of garnet analyses was carried out, while plagioclase and other major minerals were analysed to a lesser extent.

Robust regression analysis for defining predominant exchange vectors in biotites were performed using the statistical program NCSS.

Chemistry of major minerals

All analysed garnets exhibit almandine compositions containing significant amounts of pyrope and spessartine and subordinate grossular component (Table 2). The amounts of almandine and pyrope components increase, while the amounts of spessartine and grossular component decrease from core to rim in garnet grains of all investigated micaschists. All the studied micaschists contain typical ferruginous staurolite characterized by low MgO (from 0.30 to maximally 2.00 % — Erić 2005). The plagioclase of all the investigated micaschists corresponds to oligoclase (Table 3) containing 26–30 mol % anorthite. Paragonite was identified only in the CV1 variety and it is worth noting that this micaschist contains sodium-rich muscovite that is muscovite with the highest content of paragonite component (Table 3).

Representative biotite analyses of micaschist varieties from different samples are shown in Tables 4–6. All chemical analyses are normalized on the basis of 22 O assuming all Fe as Fe^{2+}. Biotites from investigated micaschists differ in their X_{Mg} values (CV1—0.57–0.62, CV2—0.47–0.50 and RH—0.52–0.57) (Fig. 8). Additionally, biotites from CV1 and RH micaschists have almost identical Ti contents ranging 0.15–0.20 and 0.13–0.22 atoms per formula unit (apfu), respectively, while biotite of the CV2 variety shows higher Ti contents (0.20–0.30 apfu). Significant within-grain (Table 6, analyses 2a–2b) and especially between grains (individual grains from different samples: analyses 3–6, 4–7) compositional variations are found only for biotites from the RH variety. Finally, biotites occurring as inclusions in CV1 variety (Table 7) display similar X_{Mg} values and significantly lower Ti contents (0.10–0.13 apfu) in comparison to matrix biotite (Table 4). The observed variability in chemical composition, particularly in Ti content and X_{Mg} values in biotite from the investigated micaschist varieties as well as in different biotite generations (CV1), can be a good opportunity for applying the Ti-in-biotite geothermometer (Henry et al. 2005) whereas the frequency of isotherms suggests that all biotites developed in the most sensitive part of the Ti–X_{Mg} diagram (Fig. 9).

Biotite crystallochemistry

Numerous studies have confirmed that the amounts of Ti incorporated in biotite depend not only on temperature, but also on the mineral assemblage, pressure and biotite crystal chemistry (Guidotti et al. 1977; Dymek 1983; Lobotka 1983; Guidotti 1984; Henry & Guidotti 2002; Henry et al. 2005).

The presence of titanium in biotite is related to substitutions in octahedral and/or tetrahedral and octahedral sites (Dymek 1983; Henry & Guidotti 2002). The substitution:

$$Ti^{4+} + 2O^{2-} + H_2 \rightarrow R^{2+} + 2OH^-$$

(where R^{2+} is a divalent octahedral cation), which represents deprotonation (dehydrogenation) through the loss of H (Waters & Charnley 2002; Cesare et al. 2003), often takes place in high-temperature metapelitic biotites. As possible substitution mechanisms to account for Ti incorporation in the investigated biotites we used the exchange vectors $Ti\square R_{-2}$ ($2^{VI}R^{2+} = {}^{VI}Ti + {}^{VI}\square$; where R^{2+} is a divalent octahedral cation and $\square$ is vacancy) and $TiRAl_{-2}$ ($2^{VI}Al = Ti + {}^{VI}R^{2+}$) for octahedral sites and $TiAl_2R_{-1}Si_{-2}$ ($2^{IV}Si + {}^{VI}R^{2+} = {}^{VI}Ti + 2^{IV}Al$) and $Al_2R_{-1}Si_{-2}$ ($^{VI}R^{2+} + {}^{IV}Si = 2^{IV}Al + 2^{VI}Al$) for substitutions between octahedral and tetrahedral sites, respectively. The direction of these exchange vectors for biotites from particular micaschist varieties was determined using the robust regression method. The obtained results are presented in Table 8 and Fig. 10a–d and all of them display statistical significance ($p < 0.001$) without taking the value R^2 into account.

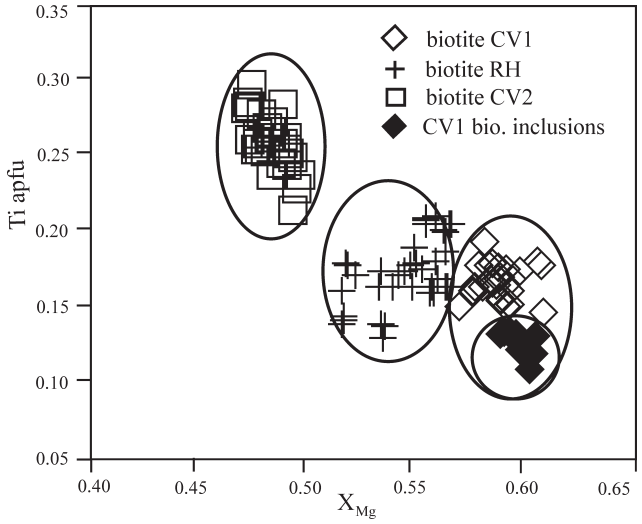

Fig. 8. Varieties of investigated micaschists with respect to Ti content and X_{Mg} values in biotites.

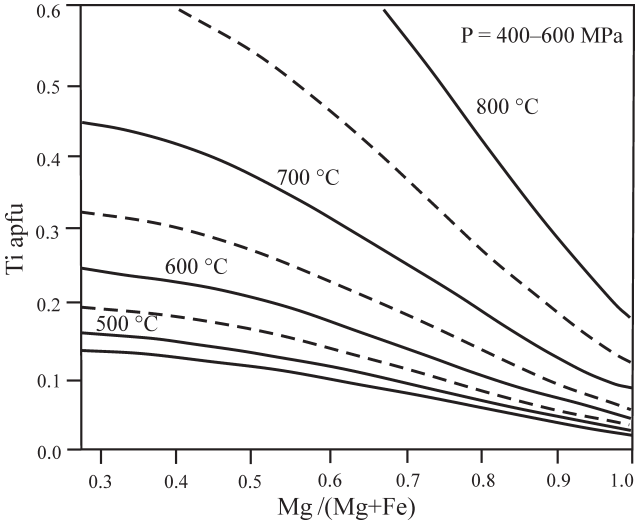

Fig. 9. Isotherms according to the Ti-in-biotite geothermometer in metapelites (Henry et al. 2005).

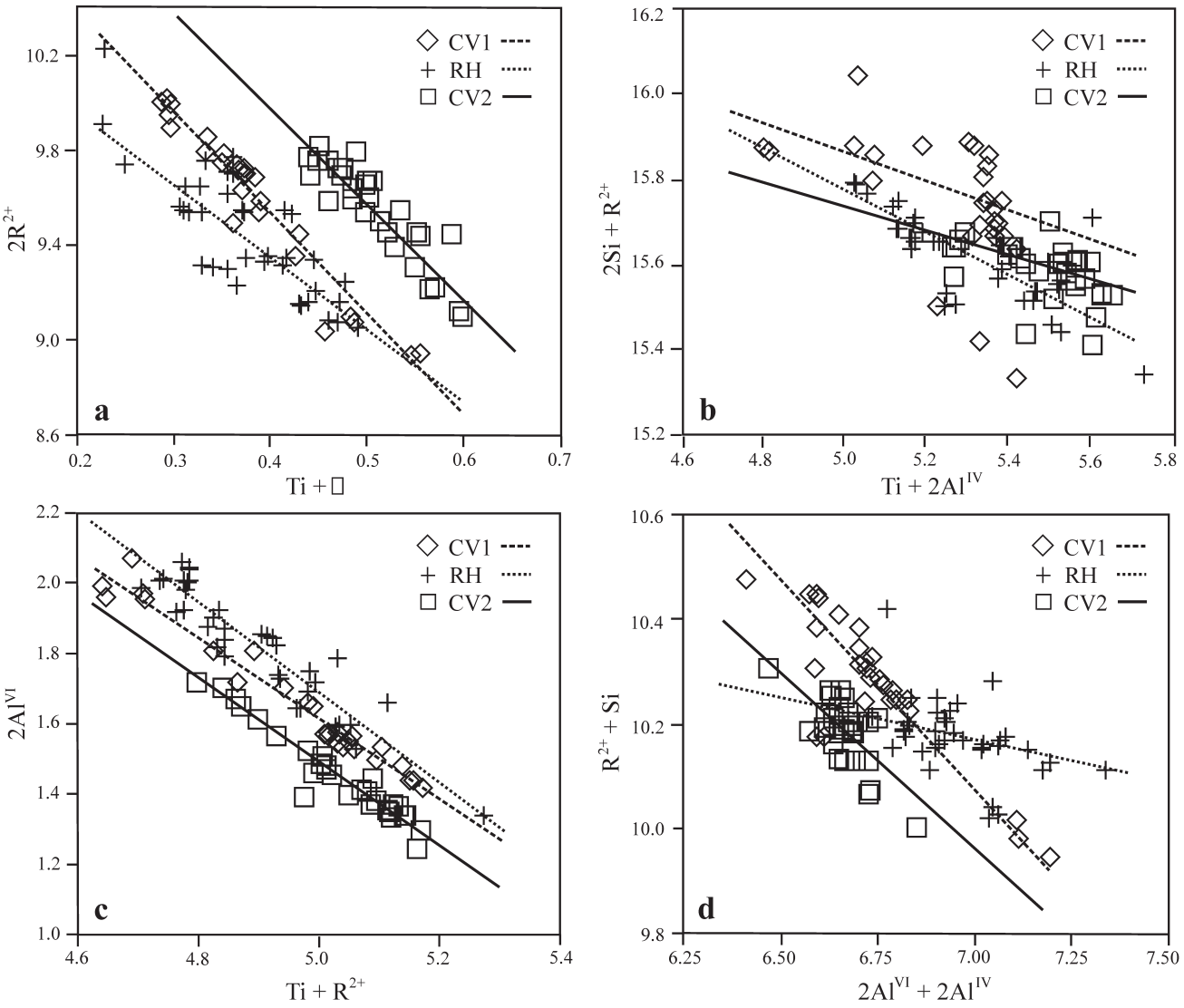

Fig. 10. Regression lines of substitutions in investigated biotites. **a** — $Ti\square R_{-2}$, **b** — $TiAl_2R_{-1}Si_{-2}$, **c** — $TiRAl_{-2}$, **d** — $Al_2R_{-1}Si_{-1}$.

Table 2: Representative microprobe analyses of garnet and biotite in the investigated micaschists.

	Garnet					Biotite			
	CV1-r	**CV2-r**	**RH-r**	**CV1-incl.**		**CV1-r**	**CV2-r**	**RH-r**	**CV1-incl.**
SiO_2	37.03	37.02	36.52	37.25	**SiO_2**	36.34	36.96	37.04	35.97
TiO_2	0.02	0.05	0.02	0.00	**TiO_2**	1.49	2.25	1.48	1.21
Al_2O_3	21.17	21.43	21.11	21.14	**Al_2O_3**	18.61	19.00	19.80	19.64
FeO	31.58	31.78	34.62	33.66	**FeO**	16.52	18.57	16.66	15.71
MnO	3.32	3.45	1.58	3.05	**MnO**	0.04	0.00	0.00	0.08
MgO	3.98	3.68	3.05	3.10	**MgO**	13.17	10.02	11.76	12.83
CaO	2.70	2.45	2.95	1.96	**CaO**	0.02	0.00	0.00	0.02
Na_2O	0.01	0.00	0.02	0.00	**Na_2O**	0.38	0.31	0.51	0.32
K_2O	0.00	0.00	0.01	0.00	**K_2O**	8.73	9.10	7.86	8.92
Sum	99.81	99.86	99.88	100.16	**Sum**	95.30	96.21	95.11	94.70
Si	2.961	2.964	2.937	2.991	**Si**	5.429	5.514	5.495	5.388
Al^{IV}	0.039	0.036	0.063	0.009	**Al^{IV}**	2.571	2.486	2.505	2.612
Al^{VI}	1.955	1.986	1.938	1.992	**Al^{VI}**	0.706	0.855	0.958	0.855
Ti	0.001	0.003	0.001	0.000	**Ti**	0.167	0.252	0.165	0.136
Fe^{3+}	0.083	0.044	0.126	0.016	**Mg**	2.933	2.228	2.601	2.865
Mg	0.474	0.439	0.366	0.371	**Fe^{2+}**	2.064	2.317	2.067	1.968
Fe^{2+}	2.028	2.084	2.203	2.244	**Mn**	0.005	0.000	0.004	0.010
Mn	0.225	0.234	0.108	0.207	**Ca**	0.003	0.000	0.000	0.003
Ca	0.231	0.210	0.254	0.169	**Na**	0.110	0.090	0.147	0.093
Na	0.002	0.000	0.003	0.000	**K**	1.664	1.732	1.488	1.705
K	0.000	0.000	0.001	0.000	**cations**	15.562	15.474	15.430	15.635
cations	7.999	8.000	8.000	7.999	**X_{Mg}**	0.587	0.490	0.557	0.593
Alm	68.5	70.2	75.1	75.0	r — rim of grain,				
Py	16.0	14.8	12.5	12.4	Alm — almandine, Py — pyrope, Sp — spessartine, Grs — grossular				
Sp	7.6	7.9	2.5	6.9	X_{Mg} = Mg/(Fe+Mg)				
Grs	3.7	4.8	3.7	4.8					

Table 3: Representative microprobe analyses of plagioclase, muscovite and paragonite in the investigated micaschists.

	Plagioclase					Muscovite				Paragonite
	CV1-r	**CV2-r**	**RH-r**	**CV1-incl.**		**CV1-r**	**CV2-r**	**RH-r**	**CV1-incl.**	**CV1-r**
SiO_2	61.28	61.25	60.83	61.20	**SiO_2**	45.34	45.28	47.16	47.00	45.09
TiO_2	0.00	0.00	0.00	0.00	**TiO_2**	0.35	0.47	0.74	0.55	0.15
Al_2O_3	24.25	24.38	24.51	24.31	**Al_2O_3**	35.54	35.64	34.47	36.32	39.00
FeO	0.00	0.00	0.03	0.00	**FeO**	2.29	1.31	3.11	0.61	0.98
MnO	0.00	0.00	0.00	0.00	**MnO**	0.03	0.00	0.03	0.14	0.00
MgO	0.00	0.00	0.00	0.00	**MgO**	0.52	0.73	1.21	1.12	0.09
CaO	6.29	6.26	5.56	6.07	**CaO**	0.02	0.01	0.00	0.00	0.31
Na_2O	8.23	8.25	8.52	8.29	**Na_2O**	2.62	0.94	1.87	1.60	6.55
K_2O	0.06	0.05	0.07	0.05	**K_2O**	7.43	9.72	8.82	8.20	1.74
Sum	100.11	100.19	99.52	99.92	**Sum**	94.14	94.10	97.41	95.54	93.91
Si	2.721	2.717	2.714	2.721	**Si**	6.079	6.089	6.617	6.151	5.900
Al	1.269	1.275	1.289	1.274	**Al^{IV}**	1.921	1.911	1.833	1.849	2.100
Ti	0.000	0.000	0.000	0.000	**Al^{VI}**	3.696	3.737	3.479	3.752	3.915
Fe	0.000	0.000	0.001	0.000	**Ti**	0.035	0.048	0.073	0.054	0.015
Mg	0.000	0.000	0.000	0.000	**Mg**	0.104	0.146	0.236	0.218	0.018
Mn	0.000	0.000	0.000	0.000	**Fe^{2+}**	0.257	0.147	0.340	0.067	0.107
Ca	0.299	0.298	0.266	0.289	**Mn**	0.003	0.000	0.003	0.016	0.000
Na	0.708	0.710	0.737	0.715	**Ca**	0.003	0.001	0.000	0.000	0.043
K	0.003	0.003	0.004	0.003	**Na**	0.681	0.245	0.474	0.406	1.662
cations	5.000	5.003	5.011	5.002	**K**	1.271	1.667	1.471	1.369	0.290
Ab	70.1	70.3	73.2	71.0	**cations**	14.050	13.991	14.526	13.882	13.557
An	29.6	29.5	26.4	28.7	**X_{Ms}**	0.651	0.872	0.756	0.736	0.148
Or	0.3	0.3	0.4	0.3	**X_{Pg}**	0.349	0.128	0.244	0.264	0.852
Ab — albite, An — anorthite, Or — orthoclase					$X_{Ms}=X_K/(X_K+X_{Na})$; $X_K=K/(K+Na+Ca)$; $X_{Na}=Na/(K+Na+Ca)$; $X_{Pg}=1-X_{Ms}$ r — rim of grain					

The directions of exchange vectors (regression lines, Fig. 10a–d) for biotites from RH micaschist crosscut the mutually sub-parallel directions of exchange vectors shown by biotites from the CV1 and CV2 varieties. These discrepancies are obvious in all cases, especially for $^{VI}R^{2+} + {}^{IV}Si = 2^{IV}Al + 2^{VI}Al$ substitution (Fig. 10d). The reason for these discrepancies is most probably related to the observed compositional variations shown by RH biotites (note that the individual biotite analyses have different weights in the regression model).

Table 4: Representative microprobe analyses of biotites in CV1 micaschists.

	Bt-1a	Bt-1b	Bt-2a	Bt-2b	Bt-3	Bt-4	Bt-5	Bt-6	Bt-7
SiO_2	36.13	36.38	36.08	36.22	36.51	37.91	38.35	35.74	37.13
TiO_2	1.43	1.47	1.57	1.52	1.40	1.37	1.40	1.56	1.46
Al_2O_3	18.79	19.13	19.15	18.95	18.64	18.36	19.53	18.55	18.73
FeO	16.62	16.43	15.73	15.94	16.45	17.06	15.66	15.83	15.90
MnO	0.07	0.04	0.12	0.07	0.04	0.05	0.09	0.07	0.12
MgO	12.67	12.56	12.79	12.78	13.24	12.67	12.77	12.51	13.02
CaO	0.02	0.01	0.03	0.00	0.02	0.00	0.00	0.06	0.00
Na_2O	0.40	0.53	0.45	0.34	0.37	0.74	0.91	0.14	0.62
K_2O	8.44	8.98	9.01	9.19	8.80	8.22	8.23	8.83	8.35
Sum	94.57	95.53	94.93	95.01	95.47	96.38	96.94	93.31	95.33
Si	5.434	5.422	5.401	5.424	5.441	5.579	5.563	5.442	5.508
Al^{IV}	2.566	2.578	2.599	2.576	2.559	2.421	2.437	2.558	2.492
Al^{VI}	0.764	0.782	0.779	0.769	0.716	0.763	0.901	0.771	0.783
Ti	0.162	0.165	0.177	0.171	0.157	0.152	0.153	0.181	0.163
Mg	2.841	2.791	2.854	2.853	2.942	2.780	2.761	2.840	2.879
Fe^{2+}	2.090	2.048	1.969	1.996	2.050	2.100	1.900	2.016	1.973
Mn	0.009	0.005	0.015	0.009	0.005	0.006	0.011	0.009	0.015
Ca	0.003	0.002	0.005	0.000	0.003	0.000	0.000	0.010	0.000
Na	0.117	0.153	0.131	0.099	0.107	0.211	0.256	0.041	0.178
K	1.619	1.707	1.721	1.756	1.673	1.543	1.523	1.715	1.580
cations	15.605	15.653	15.651	15.653	15.653	15.555	15.505	15.583	15.571
X_{Mg}	0.576	0.577	0.592	0.588	0.589	0.570	0.592	0.585	0.593
Henry et al. (2005) [T(°C)]	568	573	593	584	566	552	562	595	576
for all analyses: Ti_{apfu} sd = 0.011, X_{Mg} sd = 0.009; sd — standard deviation									

Table 5: Representative microprobe analyses of biotites in CV2 micaschists.

	Bt-1a	Bt-1b	Bt-2a	Bt-2b	Bt-3	Bt-4	Bt-5	Bt-6	Bt-7
SiO_2	36.58	37.24	35.57	35.48	35.88	35.47	35.08	35.42	35.29
TiO_2	2.11	2.36	2.23	2.45	2.36	2.39	2.13	2.24	2.09
Al_2O_3	18.56	18.92	18.52	18.78	18.74	18.60	18.62	18.61	18.42
FeO	18.84	19.01	19.89	19.70	19.40	19.53	19.34	20.08	19.84
MnO	0.00	0.00	0.04	0.04	0.04	0.07	0.04	0.13	0.01
MgO	10.39	10.19	10.27	10.12	10.14	10.22	10.37	10.20	10.36
CaO	0.00	0.00	0.00	0.00	0.02	0.01	0.00	0.02	0.00
Na_2O	0.49	0.44	0.05	0.28	0.08	0.24	0.07	0.18	0.11
K_2O	8.82	8.59	9.45	9.39	9.76	9.03	9.18	9.44	9.33
Sum	95.79	96.75	96.02	96.24	96.42	95.56	94.83	96.32	95.45
Si	5.494	5.518	5.384	5.355	5.401	5.378	5.363	5.357	5.375
Al^{IV}	2.506	2.482	2.616	2.645	2.599	2.622	2.637	2.643	2.625
Al^{VI}	0.779	0.822	0.687	0.696	0.726	0.702	0.718	0.673	0.681
Ti	0.238	0.263	0.254	0.278	0.267	0.273	0.245	0.255	0.239
Mg	2.326	2.251	2.317	2.277	2.275	2.310	2.363	2.300	2.352
Fe^{2+}	2.366	2.356	2.518	2.487	2.442	2.477	2.473	2.540	2.527
Mn	0.000	0.000	0.005	0.005	0.005	0.009	0.005	0.017	0.001
Ca	0.000	0.000	0.000	0.000	0.003	0.002	0.000	0.003	0.000
Na	0.143	0.126	0.015	0.082	0.023	0.071	0.021	0.053	0.032
K	1.690	1.624	1.825	1.808	1.874	1.747	1.790	1.821	1.813
cations	15.542	15.442	15.621	15.633	15.615	15.591	15.615	15.662	15.645
X_{Mg}	0.496	0.489	0.479	0.478	0.490	0.483	0.489	0.475	0.482
Henry et al. (2005) [T(°C)]	621	637	629	644	630	642	625	629	618
for all analysis: Ti_{apfu} sd = 0.018, X_{Mg} sd = 0.007; sd — standard deviation									

Geothermobarometry

The temperature of metamorphism for the investigated micaschists was calculated using garnet-biotite (GB) Fe-Mg exchange (Bhattacharya et al. 1992; Holdaway 2000), garnet-muscovite (GM) (Wu et al. 2002), muscovite-paragonite (MP) (Blencoe et al. 1994) and Ti-in-biotite geothermometer (Henry et al. 2005). Pressures were determined using the geobarometers based on the net-transfer reactions: anorthite-grossular-kyanite-quartz (GASP) (Powell & Holland 1988), garnet-biotite-plagioclase-quartz (GBPQ) (Wu et al. 2004a) and garnet-muscovite-plagioclase-quartz (GMPQ) (Wu et al. 2004b).

The average values of temperature and pressure based on the all above mentioned calibrations and those obtained from the THERMOCALC 3.21 program are given in Table 9.

Calculated temperatures using the Henry et al. (2005) formalism for all studied biotites are listed in Tables 4–7 and plotted on the Ti versus X_{Mg} diagram (Fig. 11a). Biotites

Table 6: Representative microprobe analyses of biotites in RH micaschists.

	Bt-1a	Bt-1b	Bt-2a	Bt-2b	Bt-3	Bt-4	Bt-5	Bt-6	Bt-7
SiO_2	37.70	38.13	37.58	37.56	35.62	35.47	35.87	37.72	38.91
TiO_2	1.58	1.65	1.49	1.72	1.26	1.55	1.78	1.92	1.93
Al_2O_3	20.02	19.53	19.51	19.70	19.94	19.41	19.39	19.52	19.93
FeO	17.57	17.33	17.35	16.67	18.30	18.05	16.55	16.59	16.86
MnO	0.00	0.11	0.08	0.18	0.00	0.02	0.08	0.00	0.09
MgO	11.64	11.72	11.38	11.37	10.94	11.55	11.96	11.82	11.73
CaO	0.00	0.00	0.00	0.00	0.04	0.00	0.04	0.00	0.14
Na_2O	0.55	0.44	0.72	0.60	0.25	0.30	0.32	0.37	0.21
K_2O	8.20	8.50	7.86	8.09	8.64	8.84	8.82	8.40	7.12
Sum	97.26	97.41	95.97	95.89	94.99	95.19	94.81	96.34	96.92
Si	5.493	5.545	5.543	5.534	5.375	5.346	5.387	5.531	5.613
Al^{IV}	2.507	2.455	2.457	2.466	2.625	2.654	2.613	2.490	2.387
Al^{VI}	0.932	0.892	0.935	0.955	0.922	0.794	0.819	0.904	1.001
Ti	0.173	0.180	0.165	0.191	0.143	0.176	0.201	0.212	0.209
Mg	2.529	2.541	2.502	2.497	2.460	2.595	2.678	2.584	2.522
Fe^{2+}	2.141	2.108	2.140	2.054	2.309	2.275	2.079	2.034	2.034
Mn	0.000	0.014	0.000	0.022	0.000	0.003	0.010	0.000	0.011
Ca	0.000	0.000	0.000	0.000	0.006	0.000	0.006	0.000	0.022
Na	0.155	0.155	0.206	0.171	0.073	0.088	0.093	0.105	0.059
K	1.524	1.577	1.479	1.521	1.663	1.700	1.690	1.571	1.310
cations	15.454	15.467	15.427	15.411	15.577	15.631	15.576	15.473	15.168
X_{Mg}	0.541	0.546	0.539	0.549	0.516	0.533	0.563	0.559	0.554
Henry et al. (2005) [T(°C)]	570	581	559	593	516	571	608	616	612
for all analysis: Ti_{apfu} sd = 0.022, X_{Mg} sd = 0.017; sd — standard deviation									

Table 7: Representative microprobe analyses of biotite inclusions in staurolite grains (CV1 micaschists).

	Bt-1	Bt-2	Bt-3	Bt-4	Bt-5	Bt-6	Bt-7	Bt-8	Bt-9
SiO_2	35.97	36.04	37.93	38.66	36.00	38.29	37.31	37.15	36.65
TiO_2	1.21	1.18	1.20	1.00	1.19	1.10	1.10	1.15	1.20
Al_2O_3	19.64	19.07	19.18	18.82	19.35	19.00	19.23	19.18	19.30
FeO	15.71	15.91	14.92	14.78	15.81	14.85	15.24	15.33	15.51
MnO	0.08	0.03	0.13	0.10	0.05	0.11	0.09	0.08	0.08
MgO	12.83	12.79	12.84	12.61	12.81	12.72	12.72	12.77	12.82
CaO	0.02	0.03	0.00	0.00	0.02	0.00	0.01	0.01	0.02
Na_2O	0.32	0.37	0.22	0.68	0.34	0.45	0.50	0.40	0.30
K_2O	8.92	8.96	8.35	8.18	8.94	8.27	8.55	8.60	8.74
Sum	94.70	94.38	94.77	94.83	94.51	94.79	94.75	94.67	94.62
Si	5.388	5.426	5.606	5.700	5.332	5.653	5.545	5.532	5.475
Al^{IV}	2.612	2.574	2.394	2.300	2.668	2.347	2.455	2.468	2.525
Al^{VI}	0.855	0.810	0.948	0.970	0.807	0.960	0.914	0.899	0.874
Ti	0.136	0.134	0.133	0.111	0.136	0.122	0.124	0.129	0.135
Mg	2.865	2.871	2.829	2.772	2.908	2.799	2.817	2.834	2.854
Fe^{2+}	1.968	2.003	1.844	1.822	2.014	1.834	1.894	1.909	1.938
Mn	0.010	0.004	0.016	0.012	0.006	0.014	0.011	0.010	0.010
Ca	0.003	0.005	0.000	0.000	0.003	0.000	0.002	0.002	0.003
Na	0.093	0.108	0.063	0.194	0.100	0.129	0.144	0.115	0.087
K	1.705	1.705	1.575	1.539	1.737	1.556	1.621	1.634	1.666
cations	15.635	15.640	15.408	15.420	15.711	15.414	15.527	15.532	15.567
X_{Mg}	0.593	0.589	0.605	0.603	0.591	0.604	0.598	0.597	0.596
Henry et al. (2005) [T(°C)]	535	529	535	485	534	512	514	522	534
for all analysis: Ti_{apfu} sd = 0.008, X_{Mg} sd = 0.005; sd — standard deviation									

from CV1 micaschist and most biotites from RH micaschist conform to the 580 °C geotherm (550–600 °C). Biotites occurring as inclusions in staurolite in CV1 micaschist exhibit lower Ti contents suggesting equilibration at lower temperatures (Fig. 11a). Temperatures calculated for biotites from CV2 micaschist range from 600° to 640 °C.

A comparison of calculated temperatures for individual micaschist varieties obtained by Ti-in-biotite and garnet-biotite geothermometers (Bhattacharya et al. 1992; Holdaway 2000) is graphically shown in Fig. 11b–d.

Discussion

The investigated micaschists from Crni vrh and Resavski humovi represent non-graphitic peraluminous metapelites with Ti-saturated minerals. Three micaschist varieties, CV1, CV2 and RH have been petrographically distinguished. The average values of different geothermobarometric methods suggest that the RH micaschist variety (Grt + St + Bt + Ms + Pl + Qtz) reached a temperature of about 550 °C and pressure of 680 MPa, while CV2 micaschists

Table 8: Results of robust regression for possible substitutions in biotites of the investigated micaschists.

Exchange vectors	x,y	CV1	CV2	RH
$Ti□R_{-2}$	$x = Ti + □$ $y = 2R^{2+}$	y = 11.216 – 4.207·x RMSE = 0.048 n = 26 **R^2 = 0.97**	y = 11.556 – 3.972·x RMSE = 0.080 n = 29 **R^2 = 0.84**	y = 10.572 – 3.048·x RMSE = 0.127 n = 37 **R^2 = 0.71**
$TiAl_2R_{-1}Si_{-2}$	$x = Ti + 2Al^{IV}$ $y = 2Si + R^{2+}$	y = 17.540 – 0.338·x RMSE = 0.072 n = 27 **R^2 = 0.38**	y = 17.116 – 0.279·x RMSE = 0.031 n = 28 **R^2 = 0.51**	y = 18.237 – 0.497·x RMSE = 0.042 n = 36 **R^2 = 0.79**
$TiRAl_{-2}$	$x = Ti + R^{2+}$ $y = 2Al^{VI}$	y = 7.274 – 1.134·x RMSE = 0.028 n = 27 **R^2 = 0.97**	y = 7.413 – 1.186·x RMSE = 0.017 n = 28 **R^2 = 0.98**	y = 8.103 – 1.286·x RMSE = 0.056 n = 37 **R^2 = 0.88**
$Al_2R_{-1}Si_{-1}$	$x = 2Al^{VI} + 2Al^{IV}$ $y = R^{2+} + Si$	y = 15.675 – 0.803·x RMSE = 0.022 n = 25 **R^2 = 0.97**	y = 14.621 – 0.670·x RMSE = 0.043 n = 29 **R^2 = 0.49**	y = 11.280 – 0.161·x RMSE = 0.025 n = 34 **R^2 = 0.40**
n — number of analyses; $y = b_o – b_1x$; R^2 — coeficient of determination; RMSE — Root Mean Square Error				

Table 9: Results of geothermobarometric analyses of micaschist from Crni vrh and Resavski humovi.

Temperature (average values) (T°C)				
References	**CV1**	**CV2**	**RH**	**CV1 incl.**
		garnet-biotite geothermometry (GB)		
Bhattacharya et al. (1992)	574 sd = 9	631 sd = 6	545 sd = 10	516 sd = 11
Holdaway (2000)	589 sd = 10	636 sd = 6	557 sd = 8	530 sd = 15
		garnet-muscovite geothermometry (GM)		
Wu et al. (2002)	590 sd = 9	640 sd = 8	548 sd = 19	550 sd = 18
		muscovite-paragonite geothermobarometry (MP)		
Blencoe et al. (1994)	600 sd = 20	–	–	–
		Ti-in-biotite geothermometry		
Henry et al. (2005)	581 sd = 14	633 sd = 11	571 sd = 32	522 sd = 16
Pressure (average values) (MPa)				
	CV1	**CV2**	**RH**	**CV1 incl.**
		garnet-plagioclase-kyanite-quartz geobarometry (GASP)		
Powell & Holland (1988)	600 sd = 50	630 sd = 60	590 sd = 60	410 sd = 60
		garnet-biotite-plagioclase-quartz geobarometry (GBPQ)		
Wu et al. (2004a) (exp. 2)	690 sd = 60	720 sd = 50	700 sd = 50	560 sd = 60
		garnet-muscovite-plagioclase-quartz geobarometry (GMPQ)		
Wu et al. (2004b) (exp. 2)	720 sd = 60	750 sd = 50	740 sd = 50	590 sd = 60
TERMOCALC 3.21				
Powell & Holland (2001)	T = 582 °C (sd = 19) P = 590 MPa (sd=120)	T = 622 °C (sd = 17) P = 620 MPa (sd = 140)	T = 548 °C (sd = 20) P = 600 MPa (sd = 160)	

(St + Grt + Bt + Ms + Pg + Pl + Qtz) were metamorphosed at 630 °C and 700 MPa (Fig. 12). The CV1 variety (St + Grt + Bt + Ms + Pg + Pl + Qtz) is characterized by the presence of two biotite and garnet generations. The first generation of garnet and biotite (which occurs as an inclusion in staurolite) revealed an average temperature of 530 °C and pressure of 520 MPa. The second generation of matrix garnet and biotite records temperatures of around 580 °C and pressures of 670 MPa. The matrix garnet and biotite formed along with continuously growing staurolite porphyroblasts. Note that for those varieties not containing kyanite the results obtained by GASP geobarometry are not included in the final calculations of pressure.

The average temperatures obtained by Ti-in-biotite thermometer of Henry et al. (2005) for biotites from CV1 and CV2 micaschists revealed uniform temperatures of 581 °C (sd = 14 °C) and 633 °C (sd = 11 °C), respectively. In addition, the calculated temperatures show very small differences in comparison to the temperatures obtained from other geothermometers (Table 9), in spite of the fact that the pressure values are higher (~700 MPa) than those (P = 400–600 MPa) used by Henry et al. (2005) in their calibration.

For biotite of the RH variety application of the Ti-in-biotite geothermometer gave an average temperature of 571 °C (sd = 32 °C). This value differs by 21 °C from the average temperature obtained by other methods, which is close to the error of the Ti-in-biotite geothermometer (Henry et al. 2005). However, a rather high standard deviation of 32 °C is related to the fact that more than one third of the analysed RH biotites (14 out of 37) displays a temperature difference in the range 85–110 °C. The largest differences were observed for calculated temperatures below 520 °C (n = 6, excluding T = 502 °C as an extreme value) and above 605 °C (n = 8) (Fig. 12). The pronounced variability of calculated

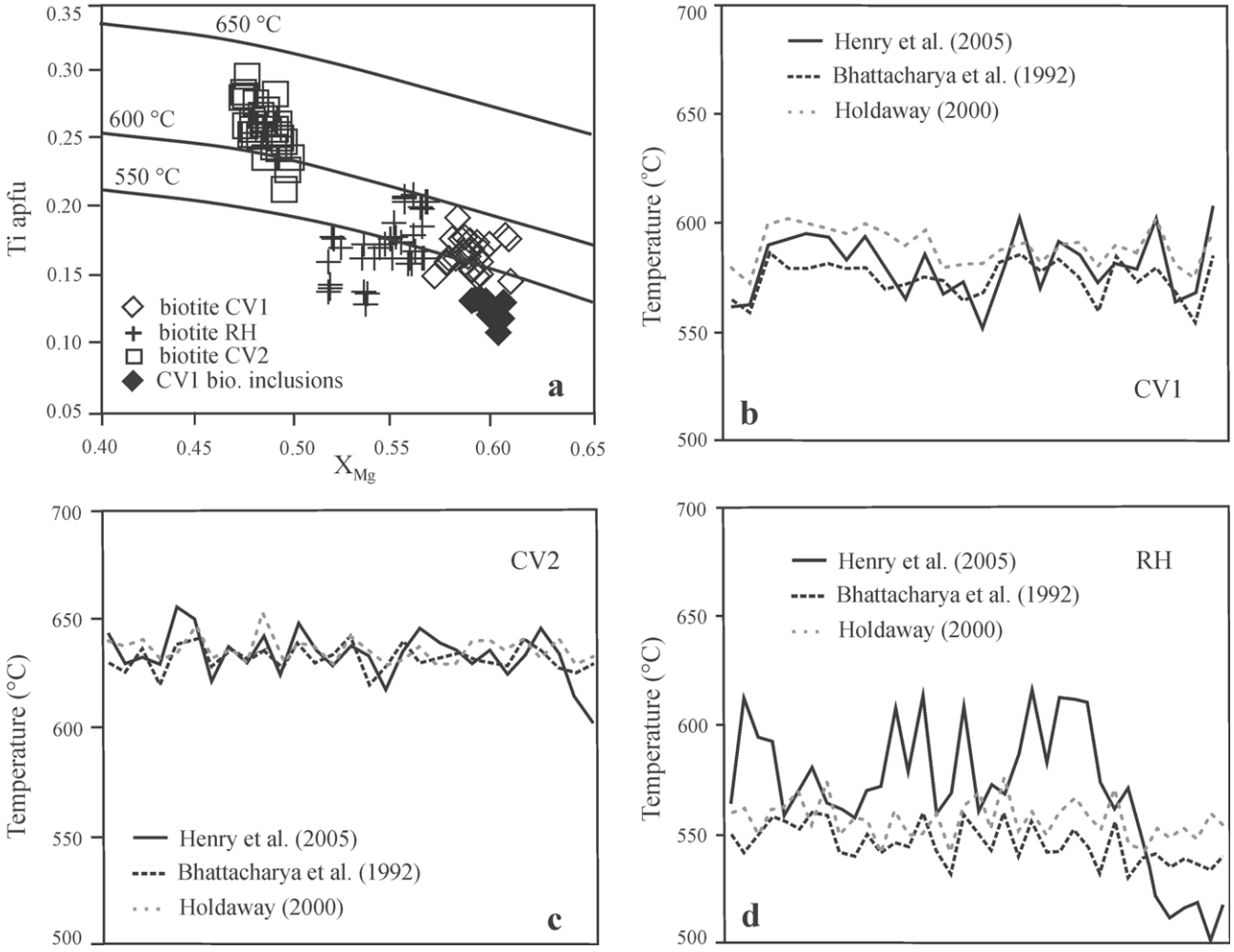

Fig. 11. **a** — Obtained temperatures according to Ti-in-biotite geothermometer. Calculated temperature values according to different geothermometers: **b** — CV1 without biotite inclusions, **c** — CV2, **d** — RH.

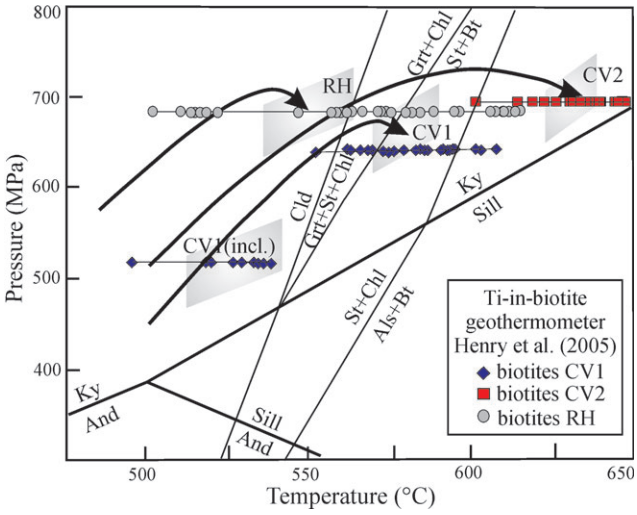

Fig. 12. PT path for investigated micaschists with temperature variations according to Ti-in-biotite geothermometer (Henry et al. 2005) and KFMASH petrogenetic grids according to Holland & Powell (1998).

temperatures for RH biotites obtained by the Ti-in-biotite method as well as differences in comparison to temperatures obtained by garnet-biotite geothermometers (Bhattacharya et al. 1992 and Holdaway 2000) are illustrated in Fig. 11d.

A greater variability of temperature estimates for RH biotites in comparison to calculated temperatures of biotites from CV1 and CV2 micaschists can be related to the problem of correlation of Ti contents and X_{Mg} values. The application of the Ti-in-biotite geothermometer generally requires low variability of Ti contents and X_{Mg} values. Biotites of CV1 micaschist (excluding the biotite inclusions in garnet) do not show correlations between Ti concentrations and X_{Mg} values, biotite of CV2 shows a negative correlation ($r = -0.67$; $p < 0.01$), whereas RH biotite exhibits a significant positive correlation ($r = 0.56$; $p < 0.01$) of these parameters. Hence, the observed positive correlation between Ti contents and X_{Mg} values in RH biotites is in disagreement with the principles of the Ti-in-biotite geothermometric method. Moreover, the method suggests that an increase in titanium concentrations should be accompanied by a decrease of Mg/(Mg + Fe) ratio (Henry et al. 2005). The positive Ti-X_{Mg} correlation is the re-

sult of the compositional variability shown by RH biotites from different samples (Table 6). Such compositional variability can be produced by the effects of chloritization or other types of alteration (Veblen & Ferry 1983) but such characteristics were not detected by optical investigations. The observed compositional variability might have been produced by temperature fluctuations during metamorphism in a relatively small area (representative samples were taken in intervals of 2–5 m). However, this possibility is not likely given the uniform results of garnet-biotite geothermometry. It is more probable that the observed compositional differences are related to compositional inhomogeneities of the pelitic protolith, with respect to Ti contents. Thus, all the analysed biotites within a single RH sample, for which temperatures above 600 °C were calculated (e.g. Table 6, analyses 5, 6 and 7), contain less iron and more titanium in octahedral position than do biotites from other RH samples.

Biotites from the CV2 variety also show variable Ti contents (Ti = 0.260, sd = 0.018 apfu) but they did not produce variations in calculated temperatures. On the contrary, the temperature estimates using the Ti-in-biotite geothermometer for CV2 biotite display a very small standard deviation of sd = 11 °C. A possible explanation can be that, as already mentioned, the composition of CV2 biotite is characterized by a negative correlation between Ti contents and X_{Mg} values. The second explanation can be that the small variations of temperature estimates are due to different sensitivity of the Ti-in-biotite geothermometer with respect to different Ti contents and X_{Mg} values. The configuration of isotherms on Henry's diagram (Fig. 2) shows that titanium concentrations above 0.25 apfu and low values of X_{Mg} produce smaller variations in calculated temperatures and this was the case of CV2 biotite. On the other hand, to obtain uniform temperature estimates for biotites that compositionally correspond to the high sensitivity field (e.g. Ti < 0.25 apfu as observed in CV1 and RH biotite) very uniform Ti contents are needed (sd < 0.02). Simultaneously, the standard deviation of X_{Mg} values should not be higher than 0.05 because it would also produce variable temperature estimates.

The high sensitivity of Ti-in-biotite with respect to Ti contents enables the calculation of temperature for two generations of biotite within individual samples of non-graphitic peraluminous metapelites. For instance, the average Ti_{apfu} value for biotite inclusions from the CV1 variety is considerably lower (0.129, sd = 0.008 apfu) than the Ti_{apfu} value for matrix biotite (Ti = 0.169, sd = 0.011 apfu) produces substantial differences in calculated temperatures of around 60 °C. It is noteworthy that similar differences are found in other geothermometric calibrations.

Conclusions

The application of the Ti-in-biotite geothermometer (Henry et al. 2005) to biotites ($Ti_{apfu} < 0.30$ and $X_{Mg} < 0.65$) from three varieties of micaschists, metamorphosed in a temperature range of 550–650 °C and at pressures of 600–800 MPa, revealed important constraints on the applicability of the method for non-graphitic peraluminous micaschists. Notable variations in calculated temperature (85–110 °C) for biotites from the RH micaschist variety are the result of a significant positive correlation between the Ti amounts and X_{Mg} values in these biotites. It can be concluded that such positive correlation should not exist within the same biotite generation and that the standard deviation for Ti contents should be less than 0.02. The biotites of two other micaschist varieties CV1 and CV2 do not show positive correlations between Ti contents and X_{Mg}, therefore, the temperature estimates based on their composition are very uniform and show close agreements with temperatures calculated by other geothermometers. The method shows high sensitivity for biotites with Ti amounts below 0.25 apfu. This enables the determination of temperature for different biotite generations which is confirmed by results from two biotite generations in CV1 micaschist revealing a temperature difference of 60 °C. Consequently, the Ti-in-biotite geothermometry can be successfully applied to similar mineral associations in non-graphitic peraluminous micaschists.

Acknowledgments: This study has been supported by the Ministry of Science of the Republic of Serbia.

References

Balogh K., Svingor E. & Cvetković V. 1994: Ages and intensities of metamorphic processes in the Batočina area, Serbo-Macedonian Massif. *Acta Mineral. Petrogr., Szeged* XXXV, 81–94.

Bhattacharya A., Mohanty L., Maji A., Sen S.K. & Raith M. 1992: Non-ideal mixing in the phlogopite-annite binary: constraints from experimental data on Mg–Fe partitioning and a reformulation of the biotite-garnet geothermometer. *Contr. Mineral. Petrology* 111, 87–93.

Blencoe G.J., Guidotti V.C. & Sassi P.F. 1994: The paragonite-muscovite solvus: II Numerical geothermometers for natural, quasibinary paragonite-muscovite pairs. *Geochim. Cosmochim. Acta* 58, 10, 2277–2288.

Cesare B., Cruciani G. & Russo U. 2003: Hydrogen deficiency in Ti-rich biotite from anatectic metapelites (El Joyazo, SE Spain): crystal-chemical aspects and implications for high-temperature petrogenesis. *Amer. Mineralogist* 88, 583–595.

Dymek R.F. 1983: Titanium, aluminium and interlayer cation substitutions in biotite from high-grade gneisses, West Greenland. *Amer. Mineralogist* 68, 880–899.

Erić S. 2005: Genesis of micaschists from Crni vrh and Resavski humovi. *PhD, Univ. Belgrade*, 1–180 (in Serbian).

Ferry J.M. & Spear F.S. 1978: Experimental calibration of the partitioning of Fe and Mg between biotite and garnet. *Contr. Mineral. Petrology* 66, 113–117.

Forbes W.C. & Flower M.F.J. 1974: Phase relations of titan-phlogopite, $K_2Mg_4TiAl_2Si_6O_{20}(OH)_4$: A refractory phase in upper mantle? *Earth Planet. Sci. Lett.* 22, 60–66.

Guidotti C.V. 1984: Micas in metamorphic rocks. In: Bailey S.W. (Ed.): Micas. *Rev. in Mineralogy*, *Mineral. Soc. Amer.*, Washington D.C., 13, 357–467.

Guidotti C.V., Cheney J.T. & Guggenheim S. 1977: Distribution of titanium between coexisting muscovite and biotite in pelitic schists from northwestern Maine. *Amer. Mineralogist* 62, 438–448.

Henry D.J. & Guidotti V.C. 2002: Ti in biotite from metapelitic rocks: Temperature effects, crystallochemical controls and pet-

rologic applications. *Amer. Mineralogist* 87, 375–382.

Henry D.J., Guidotti V.C. & Thomson A.J. 2005: The Ti-saturation surface for low to medium pressure metapelitic biotites: Implications for geothermometry and Ti-substitution mechanisms. *Amer. Mineralogist* 90, 316–328.

Holdaway M.J. 2000: Application of new experimental and garnet margules data to the garnet-biotite geothermometer. *Amer. Mineralogist* 85, 881–892.

Holland T. & Powell R. 1998: an internally-consistent thermodynamic dataset for phases of petrological interest. *J. Metamorph. Geology* 16, 309–343.

Karamata S. & Krstić B. 1996: Terranes of Serbia and neighbouring areas. The formation of the geologic frame of Serbia and the adjacent regions. In: Knežević V. & Krstić B. (Eds.): Terranes of Serbia. *Faculty of Mining and Geology,* Belgrade, 25–41.

Lobotka T.C. 1983: Analysis of the compositional variations of biotite in pelitic hornfelses from northeastern Minnesota. *Amer. Mineralogist* 68, 900–914.

Milovanović D., Marchig V. & Dimitrijević M. 1998: Petrology and chronology of the Vucje gneiss, Serbo-Macedonian massif, Yugoslavia. *Slovak Geol. Mag.* 4, 1, 29–33.

Perchuk L.L. & Lavrent'eva I.V. 1983: Experimental investigation of exchange equilibria in the system cordierite-garnet-biotite. In: Saxena S.K. (Ed.): Kinetics and equilibrium in mineral reactions. *Springer–Verlag*, 199–240.

Powell R. & Holland T.J.B. 1988: An internally consistent dataset with uncertainties and correlations. 3. Applications to geobarometry, worked examples and a computer program. *J. Metamorph. Geology* 6, 173–204.

Powell R. & Holland T. 2001: Calculating metamorphic phase equilibria. (THERMOCALC on CD-ROM).

Robert J.I. 1976: Titanium solubility in syntetic phlogopite solid solutions. *Chem. Geol.* 17, 213–227.

Veblen D.R. & Ferry J.M. 1983: A TEM study of the biotite-chlorite reaction and comparision with petrologic observation. *Amer. Mineralogist* 68, 1160–1168.

Vujisić T., Navala M., Lončarević Č., Kalenić M., Hadživuković & Milićević D. 1979: Basic geological map 1:100,000 for sheet Lapovo (L 34–139). *Federal Geol. Surv.*

Vujisić T., Kalenić M., Navala M. & Lončarević Č. 1981: Explanatory book for sheet Lapovo. Basic geological map 1:100,000. *Federal Geol. Surv.* 1–61 (in Serbian).

Waters D.J. & Charnley N.R. 2002: Local equilibrium in polymetamorphic gneiss and titanium substitution in biotite. *Amer. Mineralogist* 87, 383–396.

Wu C.M., Zhang J. & Ren L.D. 2004a: Empirical Garnet-Biotite-Plagioclase-Quartz (GBPQ). Geobarometry in medium- to high-grade metapelites. *J. Petrology* 45, N-9, 1907–1921.

Wu C.M., Zhang J. & Ren L.D. 2004b: Empirical Garnet–Muscovite–Plagioclase–Quartz (GMPQ). Geobarometry in medium-to high-grade metapelites. *Lithos* 78, 319–332.

Wu C.M., Wang X.S., Yang C.H., Geng Z.S. & Liu F.L. 2002: Empirical garnet-muscovite geothermometry in metapelites. *Lithos* 62, 1–13.